

---

Kanbar College Faculty Papers

---

2-16-2016

## Design of barrier coatings on kink-resistant peripheral nerve conduits.


Basak Acan Clements  
*The State University of New Jersey*

Jared Bushman  
*University of Wyoming*

N. Sanjeeva Murthy  
*The State University of New Jersey*

Mindy Ezra  
*The State University of New Jersey*

Christopher M. Pastore  
*Thomas Jefferson University*  
Follow this and additional works at: <https://jdc.jefferson.edu/kanbarfp>

 Part of the [Fiber, Textile, and Weaving Arts Commons](#), and the [Medicine and Health Sciences Commons](#)  
See next page for additional authors

[Let us know how access to this document benefits you](#)

---

### Recommended Citation

Clements, Basak Acan; Bushman, Jared; Murthy, N. Sanjeeva; Ezra, Mindy; Pastore, Christopher M.; and Kohn, Joachim, "Design of barrier coatings on kink-resistant peripheral nerve conduits." (2016). *Kanbar College Faculty Papers*. Paper 8.  
<https://jdc.jefferson.edu/kanbarfp/8>

This Article is brought to you for free and open access by the Jefferson Digital Commons. The Jefferson Digital Commons is a service of Thomas Jefferson University's [Center for Teaching and Learning \(CTL\)](#). The Commons is a showcase for Jefferson books and journals, peer-reviewed scholarly publications, unique historical collections from the University archives, and teaching tools. The Jefferson Digital Commons allows researchers and interested readers anywhere in the world to learn about and keep up to date with Jefferson scholarship. This article has been accepted for inclusion in Kanbar College Faculty Papers by an authorized administrator of the Jefferson Digital Commons. For more information, please contact: [JeffersonDigitalCommons@jefferson.edu](mailto:JeffersonDigitalCommons@jefferson.edu).

---

**Authors**

Basak Acan Clements, Jared Bushman, N. Sanjeeva Murthy, Mindy Ezra, Christopher M. Pastore, and Joachim Kohn

# Design of barrier coatings on kink-resistant peripheral nerve conduits

Journal of Tissue Engineering  
Volume 7: 1–14  
© The Author(s) 2016  
Reprints and permissions:  
sagepub.co.uk/journalsPermissions.nav  
DOI: 10.1177/2041731416629471  
tej.sagepub.com



Basak Acan Clements<sup>1</sup>, Jared Bushman<sup>2</sup>, N Sanjeeva Murthy<sup>1</sup>, Mindy Ezra<sup>1</sup>, Christopher M Pastore<sup>3</sup> and Joachim Kohn<sup>1,4</sup>

## Abstract

Here, we report on the design of braided peripheral nerve conduits with barrier coatings. Braiding of extruded polymer fibers generates nerve conduits with excellent mechanical properties, high flexibility, and significant kink-resistance. However, braiding also results in variable levels of porosity in the conduit wall, which can lead to the infiltration of fibrous tissue into the interior of the conduit. This problem can be controlled by the application of secondary barrier coatings. Using a critical size defect in a rat sciatic nerve model, the importance of controlling the porosity of the nerve conduit walls was explored. Braided conduits without barrier coatings allowed cellular infiltration that limited nerve recovery. Several types of secondary barrier coatings were tested in animal studies, including (1) electrospinning a layer of polymer fibers onto the surface of the conduit and (2) coating the conduit with a cross-linked hyaluronic acid-based hydrogel. Sixteen weeks after implantation, hyaluronic acid-coated conduits had higher axonal density, displayed higher muscle weight, and better electrophysiological signal recovery than uncoated conduits or conduits having an electrospun layer of polymer fibers. This study indicates that braiding is a promising method of fabrication to improve the mechanical properties of peripheral nerve conduits and demonstrates the need to control the porosity of the conduit wall to optimize functional nerve recovery.

## Keywords

Peripheral nerve, nerve regeneration, nerve conduit, braided conduit, braiding, porosity, hyaluronic acid

Received: 7 October 2015; accepted: 28 December 2015

## Introduction

Synthetic nerve conduits have been developed over the past 50 years as an alternative to autologous nerve grafts for repairing peripheral nerve lesions that cannot effectively be bridged using end-to-end neuroorrhaphy. At least, seven different synthetic nerve guidance conduits have been approved for clinical application in the United States, but autografts continue to be preferred for repairing nerve gaps longer than 4 cm.<sup>1,2</sup> Synthetic conduits have been found to fail because of swelling and reduction of luminal volume,<sup>3</sup> suture pull-out,<sup>4,5</sup> collapse,<sup>6</sup> and lack of mechanical strength to withstand the traction of moving joints.<sup>7</sup> Here, we report on our study of braided conduits, which have significantly improved mechanical strength and a very high degree of kink-resistance.

Braiding has been used to fabricate vascular stents,<sup>8,9</sup> but there have only been a few reports on braided nerve

conduits,<sup>10–18</sup> and none of the conduits in clinical use in the United States are braided. Since braided vascular stents were shown to possess excellent mechanical strength and flexibility,<sup>19,20</sup> we expected braiding to impart favorable

<sup>1</sup>New Jersey Center for Biomaterials, Rutgers, The State University of New Jersey, Piscataway, NJ, USA

<sup>2</sup>School of Pharmacy, University of Wyoming, Laramie, WY, USA

<sup>3</sup>Kanbar College of Design, Engineering and Commerce, Philadelphia University, Philadelphia, PA, USA

<sup>4</sup>Department of Chemistry and Chemical Biology, Rutgers, The State University of New Jersey, Piscataway, NJ, USA

### Corresponding author:

Joachim Kohn, New Jersey Center for Biomaterials, Rutgers, The State University of New Jersey, 145 Bevier Road, Piscataway, NJ 08854, USA.  
Email: kohn@rutgers.edu



mechanical properties to nerve conduits as well. Braided conduits are fabricated by first generating small diameter fibers that are either used individually or twisted together to form multi-filament yarns. The fiber or yarn is loaded into the carriers of a braiding apparatus, which travel in an interlacing pattern around a center point and wrap the fibers around a mandrel to generate a tubular conduit. Braiding may be performed using a variety of braiding parameters, patterns and angles, which determine the physical and mechanical characteristics of the final braid, along with the mandrel diameter which determines the tube's inner diameter and the individual fiber or yarn diameter which determines the thickness of the conduit walls. Once suitable fibers are available, braided conduits can be rapidly and reproducibly fabricated without dimensional limitations.

Our studies were conducted using a tyrosine-derived polycarbonate to generate the fibers via melt extrusion. The library of tyrosine-derived polycarbonates encompasses over 10,000 polymers with a wide range of properties and applications in tissue regeneration and drug delivery.<sup>21–24</sup> For the studies described here, we selected a single polymer composition, poly(desaminotyrosyl-tyrosine ethyl ester carbonate). This polymer, referred to as poly(DTE carbonate) and abbreviated as “E0000,” is a derivative of naturally occurring tyrosine dipeptide, and degrades very slowly *in vivo* releasing non-toxic diphenolic monomers and requiring over 1 year before significant changes in molecular weight are apparent.<sup>25,26</sup> Conduits composed of E0000 will therefore experience only negligible degradation within the time span of our studies and effectively remove degradation as a variable in conduit performance.

Three research groups have previously reported on the testing of braided nerve conduits *in vivo*. Nakamura and colleagues<sup>10–12,18,27,28</sup> have developed conduits braided from poly(glycolic acid) (PGA) fibers and coated with collagen (PGA-c-tube) since 1995. These conduits were used to repair 10–80 mm long nerve defects in cats and dogs, have been in clinical use in Japan since 2002, and were successfully used to treat Complex Regional Pain Syndrome Type II in two human patients.<sup>13</sup> This group later incorporated poly(L-lactic acid) fibers into the PGA braid structure (PLLA/PGA-c-tube) to address the premature degradation and loss of mechanical properties of the PGA-c-tube, and demonstrated improved outcomes in a 40 mm canine model.<sup>14</sup> Ramakrishna and coworkers separately reported favorable *in vitro* cytocompatibility and swelling behavior with conduits braided from poly(lactico-glycolic acid) (PLGA) or chitosan fibers.<sup>15</sup> These conduits showed 90% success in bridging a 12 mm gap in the rat sciatic nerve after 1 month.<sup>16</sup> Finally, Lu et al.<sup>17</sup> evaluated peripheral nerve regeneration in the 10-mm rat sciatic nerve model using poly(lactic acid) (PLA) fiber-reinforced conduits. Using twisted PLA multi-filaments, they braided

single, double, or triple-layered conduits to obtain smaller pore size with each additional layer. An 8-week *in-vivo* study did not show any differences in electrophysiology and histology due to the different layers. While these reports showed the promise of braided nerve conduits, they did not address the relationship between conduit pore size and resulting tissue infiltration or the longer-term outcomes of nerve regeneration with these conduits.

Studies of the effect of conduit pore size on the outcome of nerve regeneration have shown the optimal pore size for conduits to be in the 5–30  $\mu\text{m}$  range to enable nutrient and waste diffusion and minimize fibrotic and inflammatory cell infiltration.<sup>29–31</sup> However, considerable variation in outcomes has been reported in studies using conduits that differ in composition, method of fabrication, and the animal model used to test the conduits. It is important to note that most studies *in vivo* are performed in mice or rats where the conduit length is usually around 10 mm only. It is generally agreed that porosity will play an increasingly important role if conduits are to be used in bridging longer nerve gaps where diffusion from the termini of the conduits will limit nutrient exchange.

We found that variations in braiding lead to significant changes in the porosity of the conduits, resulting in macroporous structures. We also show that modulating conduit porosity has a significant effect on *in-vivo* nerve regeneration outcomes. Our work serves as an evaluation of kink-resistant braided conduits and accompanying barrier coatings and demonstrates that braiding, in combination with the control of conduit wall porosity is a promising, but largely overlooked approach for the development of improved synthetic nerve conduits.

## Materials and methods

### *Polymer synthesis and characterization*

Poly(DTE carbonate), E0000, was synthesized and purified utilizing previously published procedures.<sup>26</sup> Molecular weights (number average,  $M_n$ ; weight average,  $M_w$ ) and polydispersity index (PDI) were determined using gel permeation chromatography (GPC; Waters Corporation, Milford, MA) relative to polystyrene standards in dimethylformamide containing 0.1% trifluoroacetic acid as the mobile phase. The glass transition temperatures ( $T_g$ ) of the polymers were determined as described before.<sup>32</sup> E0000 used to fabricate braided conduits and dipcoated conduits had a  $M_n$  of 167,700 Da with a PDI of 1.47 and  $T_g$  of 96.5°C. The electrospun coatings were fabricated using E1001(1k), a copolymer consisting of 89 mol% DTE, 10 mole percent desaminotyrosyl-tyrosine (DT), and 1 mol% 1 kDa poly(ethylene glycol) (PEG). E1001(1k) was synthesized using previously published procedures<sup>33</sup> and had a  $M_n$  of 239,000 Da with a PDI of 1.6 and  $T_g$  of 97.0°C.

## Conduit fabrication

Different braid designs were initially implemented using 60  $\mu\text{m}$  thick industrial polypropylene (PP) prototype yarn (ATEX Technologies Inc, Pinebluff, NC) to determine the effect of braid pattern and fiber density on the conduit pore size and mechanical properties (not shown).

Braided conduits used for in-vitro and in-vivo tests were fabricated by tubular braiding of E0000 fibers. E0000 was melt extruded using a 3/8 inch single-screw extruder (Microextruder; Randcastle, Cedar Grove, NJ) and extruded fiber diameter was monitored using a laser micrometer (Z-Mike 1200 series, Groß-Umstadt, Germany). The final extruded fiber diameter ranged between 80 and 110  $\mu\text{m}$  and the post fabrication  $M_n$  was 138,550 Da with a PDI of 2.05. Three polymer fibers were then twisted together to form a multi-filament yarn and spooled onto braiding spindles. A Herzog NG 1/24-120 tubular braiding machine (Herzog Maschinenfabrik, Oldenburg, Germany) equipped with 24 carriers was used to braid conduits in a 2/2 braid pattern, over a Teflon mandrel with an outer diameter of 1.5 mm (Applied Plastics Co., Inc., Norwood, MA). After braiding, conduits were cut to desired lengths and ends were trimmed and sealed using a thermocutter (ZTS 20; AZ Zangl, Germany). Conduits were cleaned by sequential washes in cyclohexane (1 $\times$ ), 0.5 volume percent Tween20 in deionized water (1 $\times$ ), and distilled (DI) water (5 $\times$ ) while being sonicated.

To control conduit porosity, secondary electrospun layers were formed on the braided conduits on rotating mandrels in an electrospinning setup using a high voltage power supply (Gamma High Voltage Research Inc., Omaha Beach, FL) and a syringe pump (KD Scientific, Holliston, MA) connected to blunt tipped 23G stainless steel needles via 20 gauge  $\times$  3' Teflon tubing (both from Hamilton Company, Reno, NV). Polymer (10% (w/v)) solution of E1001(1k) was prepared in glacial acetic acid (Fisher Scientific, Pittsburgh, PA) using a 1:25 ratio of trans-4-hydroxy-L-proline (tHyp):E1001(1k) to eliminate beading from the electrospun fibers.<sup>34</sup> Conduit external diameter was periodically measured with calipers and electrospinning was continued until a 300  $\mu\text{m}$  thick coating was formed around the braided conduits. Conduits were thoroughly dried in the fume hood to remove residual solvent.

Alternatively or in combination with electrospun polymer coating, sterile braided conduits were also dipcoated in a 1% (w/v) sterile thiol-modified hyaluronan solution (HyStem) followed by immediate cross-linking by dipcoating in a sterile 1% (w/v) poly(ethylene glycol diacrylate) (PEGDA) solution (both from Glycosan Biosystems-BioTime, Inc. Alameda, CA) in a sonicated water bath. Conduits were dried for 5 min after each dipcoating step and the process was repeated for a total of five times. Conduits with dual electrospun and hyaluronic acid (HA) coating were fabricated by first depositing the

electrospun layer on the braided conduits as described above, followed by dipcoating in hyaluronan and PEGDA solutions. HA-coated conduits were dried overnight in the laminar flow hood and implanted in dry state for in-vivo experiments.

Dipcoated conduits were fabricated as controls via dipcoating from a 20% (w/v) E0000 solution in methylene chloride using previously published procedures,<sup>35</sup> and deposited on 1.5 mm OD teflon-coated mandrels.

To reduce the bioburden, all conduits were exposed to UV irradiation for 40 min prior to in-vivo use.

## Scanning electron microscopy

Pore size and topography of sputter-coated (SCD 004 sputter coater, 30 mA for 120 s with Au/Pd) specimens were evaluated using scanning electron microscopy (SEM; Amray 1830I, 20 kV). Pore size, braid angle and wall thickness of conduits, and the fiber diameter of electrospun mats were measured on SEM images using ImageJ (public domain software from National Institutes of Health). Braid angle was measured between a line perpendicular to the longitudinal axis of the braid and a line parallel to the groups of fibers aligned close to the tube-axis.

## Mechanical testing

Mechanical properties of braided conduits were characterized by compressive and three-point bending tests using a Syntec 5/D mechanical tester, and tensile tests using a MTS Tytron™ 250 Microforce Testing System (both from MTS, Eden Prairie, MN). Samples were preconditioned by incubation in phosphate-buffered saline (PBS) at 37°C overnight and tested immediately after removal from the incubator. Compression tests were performed on 1 cm long conduits, with a transverse crosshead speed of 6 mm/min to the endpoint displacement equivalent to 60% of initial conduit diameter. The compressive stiffness was calculated from the slope of the linear region in the force versus displacement curves. Three-point bending tests were performed on 1.5 cm long conduits placed on the lower holder beams of the bending apparatus, which were set 1 cm apart. The third point was lowered from above the midpoint of the conduit at a crosshead speed of 10 mm/min. Bending stiffness (EI) was calculated using the formula  $EI = (F/d) (L^3/48)$ , where  $F/d$  is the slope of the linear region in the force versus displacement curves and  $L = 10$  mm is the beam separation. For tensile testing, 3 cm long conduits were secured in the grips, with a grip separation of 2 cm and stretched at a speed of 20 mm/min until failure. The tensile stiffness was similarly calculated from the slope of the linear region in the force versus displacement curves. Kink tests were performed by bending 3 cm long conduits on a flexible 0.6 mm diameter wire (Applied Plastics Co., Inc.) until a kink occurred, which was defined as visually

detectable reduction in the conduit outer diameter at the point of bending. E0000 conduits fabricated by braiding and dipcoating as well as commercially available NeuraGen® conduits (Integra LifeSciences Corporation, Plainsboro, NJ) were bent and kink formation at the bending point was observed. The angle between the bent arm of the conduits and the horizontal axis was measured and reported as the bending angle. For braided conduits, kink test was carried out further by bending the conduit in a loop until a kink occurred. For this test, braided conduits were gradually twisted into smaller loops and photographed at each increment. The perimeter of the inner loop formed by the conduit was then measured using ImageJ software and the corresponding internal loop diameter was calculated from the perimeter, assuming a circular loop.

### *In-vivo evaluation*

All experiments were conducted under an approved protocol of the Rutgers Animal Care and Facilities Committee and the Institutional Animal Care and Use Committee (IACUC).

**Subcutaneous implantation of braided conduits.** Male Sprague-Dawley rats weighing 250–300 g (Charles River Labs, Wilmington, MA) were anesthetized by intraperitoneal injection of ketamine/xylazine (75/10 mg/kg, respectively) and braided conduits were implanted in four subcutaneous pockets on the animals' backs. Animals were sacrificed 3 weeks after implantation, and conduits were explanted with the surrounding connective tissue. Immediately after explantation, conduits were fixed in 10% buffered formalin, followed by tissue processing and paraffin embedding for histological staining. 6  $\mu$ m sections were prepared and stained with hematoxylin and eosin (H&E) using standard methods.

**In-situ implantation of conduits in the 1-cm rat sciatic nerve model.** Female Lewis rats weighing 200–250 g (Charles River Labs) were anesthetized by intraperitoneal injection of ketamine/xylazine (75/10 mg/kg, respectively) and implanted with conduits, using published protocols.<sup>36,37</sup> For the conduit groups, a 5 mm section of the sciatic nerve was removed and the nerve stumps were allowed to retract to form a 10 mm gap. Sterile conduits (1.2 cm long and 1.5 mm in diameter) were then sutured to the nerve stumps using two 9-0 epineurial sutures on each end, maintaining the 10-mm gap between the stumps. In the case of autografts, a 1 cm segment of nerve was removed, reversed, and sutured back in the gap using three to four 9-0 sutures on each end.

**Electrophysiology.** Recovery of the electrophysiological function after nerve injury was evaluated under general anesthesia by measuring the compound muscle action

potentials (CMAPs) at the dorsal and plantar foot muscles, which are the most distal targets of the peroneal and tibial branches of the sciatic nerve.<sup>37</sup> CMAPs were recorded immediately before surgery (intact animals) and every 4 weeks after surgery using the VikingQuest EMG system (Natus Medical Inc., San Carlos, CA). Subcutaneous electroencephalogram (EEG) needles were used as recording, reference, and ground electrodes. Reference and ground electrodes were placed at the lateral side 5th metatarsal and heel calcaneus, respectively, on the operated side of the rat. Recording electrode was inserted subcutaneously on the dorsal foot muscle over the 3rd metatarsal for the peroneal CMAP, and on the plantar muscle for the tibial CMAP. The sciatic nerve was stimulated percutaneously using a bipolar stimulating electrode at the ankle level directly posterior to the tibia. Electrodes were adjusted locally to produce maximal CMAP amplitude and the stimulus was increased incrementally to produce a supramaximal response. The average of three consecutive CMAP amplitudes, measured from the onset of the CMAP signal to the top of the peak, and three consecutive latencies were calculated for each animal and averaged for the animals in the same treatment group for plotting.

**Histomorphometric analysis of explanted nerves.** Sixteen weeks after surgery, rats were deeply anesthetized using ketamine/xylazine anesthesia, the sciatic nerve on the operated side was exposed and in-situ fixation of the nerve was performed by immersing the nerve in Trump's fixative for 30 min. The nerve was then harvested and processed as described previously.<sup>36</sup> Total numbers of myelinated axons per nerve cross-section were counted using ImageJ 1.43u software, by counting a minimum 500 myelinated axons in random 100 $\times$  images for each 1  $\mu$ m thick nerve section and averaging over three replicate nerve sections. The raw tissue area, cross-sectional area of the myelinated nerve cable, and the % nerve regeneration were measured on the 10 $\times$  images and analyzed with ImageJ 1.43u software. Axonal (inside the myelin sheath) and nerve fiber (including the myelin sheath) diameter were measured in three random 100 $\times$  samples from each section to calculate the G-ratio.<sup>38</sup>

**Muscle harvest.** Upon nerve harvest, animals were euthanized by CO<sub>2</sub> asphyxiation. The tibialis anterior (TA) and gastrocnemius muscles of both hind limbs (healthy and operated side) were immediately harvested by exposing the musculature via a knee to ankle longitudinal skin incision. The muscles were harvested from origin to insertion and weighed with an electronic balance.

### *Statistical methods*

Data in this study are represented as mean  $\pm$  SE unless otherwise indicated. One-way analysis of variance (ANOVA) tests with Dunnett's post hoc tests were used in this study

**Table 1.** Comparison of physical properties of braided conduit variations.

	Single-fiber 2/2 PP braid	Three-fiber triaxial PP braid	Three-fiber 2/2 PP braid	Three-fiber 2/2 E0000 braid
Braid angle	39.0 ± 0.9	47.4 ± 3.4	40.0 ± 1.0	41.8 ± 0.4
Pore size (µm)	59.3 ± 14	15.2 ± 3.7	45 ± 8.1	65.0 ± 19.5

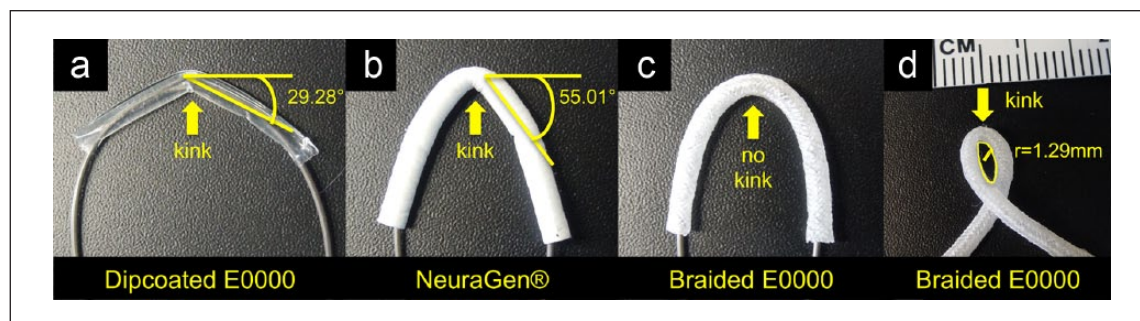


**Figure 1.** Kink tests were performed on the (a) dipcoated E0000, (b) NeuroGen®, and (c, d) braided conduits by bending the conduit on a flexible 0.6mm diameter wire until a kink in the lumen occurred. For the dipcoated conduits and NeuroGen®, a visible collapse in lumen diameter occurred when the conduit was bent at 29.28° and 55.01°, respectively, from the horizontal axis. Braided conduits resisted kinking, maintained constant lumen diameter when bent at large angles, and resumed their original shape when the load was released, while dipcoated and Neurogen conduits partially or completely occluded the lumen when bent and did not resume their original shape. Braided conduits displayed a reversible kink when bent into a loop with a corresponding radius of curvature of 1.29 mm.

to assess significant differences. Statistical significance was defined as  $p < 0.05$ .

## Results and discussion

### Conduit fabrication and physical characterization

There are many variables for braiding, which can have significant effects on the physical and mechanical features of braided devices.<sup>8,39</sup> We first explored three conduit prototypes by varying the number of filaments and twists in a yarn using commercially available non-degradable PP prototyping fibers. The resulting conduits indeed showed substantial differences in physical characteristics, such as pore size and braid angle (Table 1). The 2/2 braid constructed from three-fiber yarn had the most favorable mechanical features, demonstrating superior kink-resistance and elastic deformation. In contrast, triaxial braids were stiffer and exhibited undesirable shape memory upon deformation. Owing to a combination of pore size and mechanical properties, we explored the traditional 2/2 braiding method in more detail using E0000 fibers with diameters of 80–110 µm. The resulting conduits had an average pore size of  $65 \pm 19$  µm and an inner lumen diameter of 1.5 mm.

### Mechanical properties of braided conduits

Nerve conduits must not collapse<sup>6</sup> and retain mechanical stability to withstand the traction of moving joints.<sup>7</sup> For the

repair of large nerve gaps in areas of high mobility, flexibility and prevention of kinking are important conduit design criteria. We compared the mechanical properties of braided E0000 conduits, non-porous dipcoated E0000 conduits with  $183 \pm 15$  µm thick walls, and the clinically used NeuroGen® conduits consisting of collagen I (Integra Lifesciences, South Plainfield, NJ).<sup>40,41</sup> Due to the inability to secure a sufficient quantity of the NeuroGen® conduits, not all experiments could be replicated with these conduits and the previous findings of Yao et al.<sup>42</sup> using these conduits are cited to complete the comparison.

Kink tests were performed to assess the angle to which the E0000 conduits can be bent before any luminal occlusion occurs. Conduits were bent on a wire until a kink occurred (Figure 1). For the dipcoated conduits and NeuroGen®, a visible decrease in lumen diameter occurred when the conduits were bent 29.3° and 55.0°, respectively, from the horizontal axis (Figure 1(a) and (b)). Braided conduits resisted kinking, maintaining constant lumen diameter when bent at angles exceeding 125° (Figure 1(c) and (d)). Braided conduits also resumed their original shape after release of the load, whereas dipcoated and NeuroGen® conduits did not resume their original shape.

These results indicate that our braided conduits are highly resistant to luminal occlusion and are much more likely to maintain an open lumen when applied in areas of high flexation. The large flex angles allowed by the braided conduits are physiologically relevant; elbow, knee, and finger joints routinely bend at high angles well in excess of 90°. Failure due to breakage near the knee joint has been

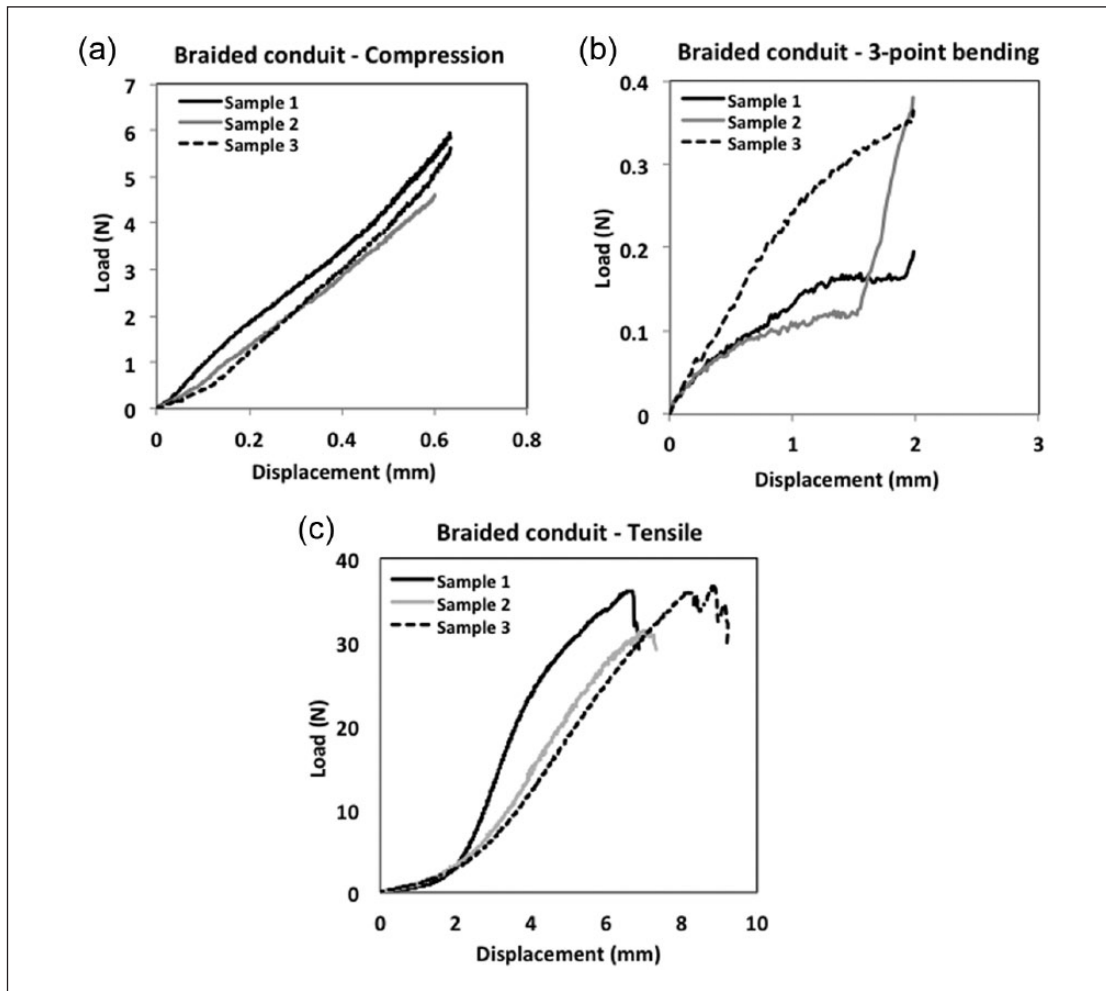


**Figure 2.** Representative load (N) versus displacement (mm) curves for (a) compression, (b) three-point-bending, and (c) tension and testing of E0000 braided conduits.

**Table 2.** Compressive structural stiffness, bending stiffness, tensile structural stiffness and ultimate tensile strength calculations for the dipcoated E0000, NeuraGen<sup>®</sup> and braided E0000 conduits (mean  $\pm$  SD of three samples tested).

	Dipcoated	NeuraGen <sup>®</sup>	Braided
Compressive structural stiffness (N/mm)	34.6 $\pm$ 2.57	0.92 $\pm$ 0.15 (Yao et al.) <sup>a</sup>	9.4 $\pm$ 0.58
Bending stiffness (EI, N mm <sup>2</sup> )	22.16 $\pm$ 0.54	N/A <sup>a</sup>	5.69 $\pm$ 0.25
Tensile structural stiffness (N/mm)	166.71 $\pm$ 41.09	2.38 $\pm$ 0.86 (Yao et al.) <sup>a</sup>	1.27 $\pm$ 0.03
Ultimate tensile strength (N)	43.46 $\pm$ 10.61	6.89 $\pm$ 2.6 (Yao et al.) <sup>a</sup>	34.7 $\pm$ 3.05
Kink angle (°)	29.28	55.01	127.60

<sup>a</sup>Data from Yao et al. are tabulated as comparison for the NeuraGen conduits due to limited supply of NeuraGen conduits for this study.

reported for 22 mm long collagen tubes that were used in the rat sciatic nerve injury model due to insufficient flexibility of tubular constructs.<sup>43</sup>

Results of quantitative mechanical tests for the braided conduits are shown in Figure 2 and compared to dipcoated and NeuraGen<sup>®</sup> conduits in Table 2. In transverse compression, the dipcoated conduits displayed the most resistance to the applied load but plastically deformed when compressed

to 60% of the inner diameter, while the braided conduits regained their original shape immediately after removing the compressive load. The reported data of the NeuraGen<sup>®</sup> conduits indicate that under compression, these conduits (compressive stiffness: 0.92  $\pm$  0.15 N/mm) deform 10-fold more than the braided conduits (compressive stiffness: 9.4  $\pm$  0.58 N/mm).<sup>42</sup> Similar trends were noted for three point-bending experiments for dipcoated (bending stiffness



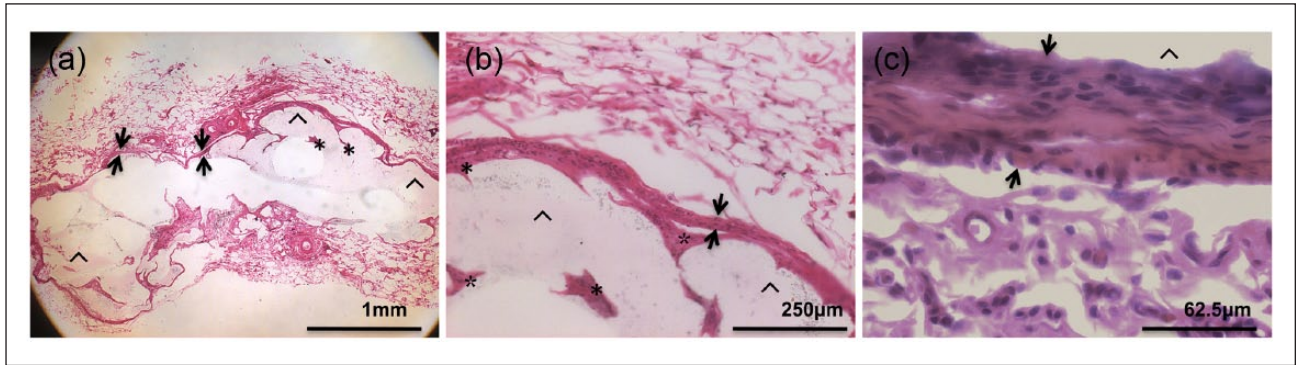


**Figure 3.** Cross-sectional view of E0000 braided conduit after 3 weeks of subcutaneous implantation in rats. Hematoxylin and eosin stained section where  $\wedge$  marks the conduit, arrows mark the fibrous capsule, and asterisk mark the infiltrating tissue. (a) 2.5 $\times$  magnification showing the cross-section of the entire conduit and surrounding tissue, (b) 10 $\times$  magnification showing the close-up view of the braided conduit fibers (lower half of the image), the fibrous capsule, and surrounding tissue, and (c) 40 $\times$  magnification showing the thickness of the fibrous capsule.

22.16 $\pm$ 0.54N/mm) and braided (bending stiffness 5.69 $\pm$ 0.25N/mm) conduits, with dipcoated conduits showing greater resistance to bending. No bending data were reported for NeuraGen<sup>®</sup> conduits. The fact that braided conduits can freely bend, without occluding their lumen, is a critical advantage over the other conduits that are either too stiff to bend, and thus may cause tissue damage, or result in a kink at the bending point, crushing the newly formed nerve cable. In terms of tensile stiffness, braided (tensile stiffness: 1.27 $\pm$ 0.03N/mm) and NeuraGen<sup>®</sup> (tensile stiffness: 2.38 $\pm$ 0.86N/mm) conduits were more compliant and yielded more readily to tension than the dipcoated (tensile stiffness: 166.71 $\pm$ 41.09N/mm) conduits. The braided conduits deformed elastically under physiological loading conditions, which is beneficial for nerves that experience movement and tensile stress. On the other hand, the ultimate tensile strength (UTS) of the braided conduits (UTS: 34.7 $\pm$ 3.05N/mm) was 5-fold higher than NeuraGen<sup>®</sup> (UTS: 6.89 $\pm$ 2.6N/mm) demonstrating the strength of the braided structure as compared to NeuraGen<sup>®</sup>. Peripheral nerves experience tensile, compressive, and shear forces created by the limb movement and muscular contraction.<sup>44,45</sup> Synthetic nerve conduits need to tolerate these forces while protecting the regenerating nerve from damage. Peripheral nerves are under tensile loads in situ and experience  $\sim$ 11% strain in resting position<sup>46,47</sup> while tolerating 11.7MPa maximum tensile stress.<sup>48</sup> Therefore, any nerve conduit that acts to bridge a peripheral nerve gap should be able to reversibly elongate under loads up to 11.7MPa. We found this load is within the linear portion of the stress–strain curve of the E0000 braided conduits, which show 17%–22% reversible strain under this load, sufficient to withstand the stress of limb movements (Figure 2(c)).

### Host response

A small control study was conducted to ensure that the conduit material does not elicit a strong inflammatory

response that could affect the results obtained in the subsequent nerve regeneration studies. To evaluate the gross tissue response, E0000 braided conduits were implanted into subcutaneous pockets on the backs of adult rats. After 3 weeks, conduits were removed and H&E histology was performed. Sections revealed the expected formation of a fibrous capsule around the conduits (Figure 3). Capsule tissue was diffusely organized and lacked a high concentration of inflammatory cells, indicating that the host response to the E0000 braided conduit was minimal and in agreement with previous findings on the host response to polymers within the family of tyrosine-derived polycarbonates.<sup>33,49</sup>

A pilot 4-week study to evaluate the effectiveness and tolerance of barrier coatings consisting of HA, alginate, or agarose hydrogels on braided conduits was also performed. Gross morphological and histological analysis on the explanted conduit and the surrounding tissues showed no signs of adverse tissue reaction when PEGDA cross-linked HA hydrogels were used as a barrier coating on the braided conduits (not shown).

Electrospun E1001(1k) mats, also used as secondary barrier coatings on the braided conduits, were not expected to invoke a host immune response, owing to the established use of this material in a number of tissue regeneration applications,<sup>21,23,35</sup> and hence were not tested in this study for inflammatory response.

### Secondary coatings

The H&E stain in Figure 3 also revealed that surrounding tissue penetrated through the pores and entered into the E0000 conduit lumen. Effects of conduit pore size on the outcome of nerve regeneration have been investigated and, while results and interpretations of this critical aspect vary widely, the optimal pore size for conduits was reported to be in the 5–30 $\mu$ m range to enable nutrient and waste

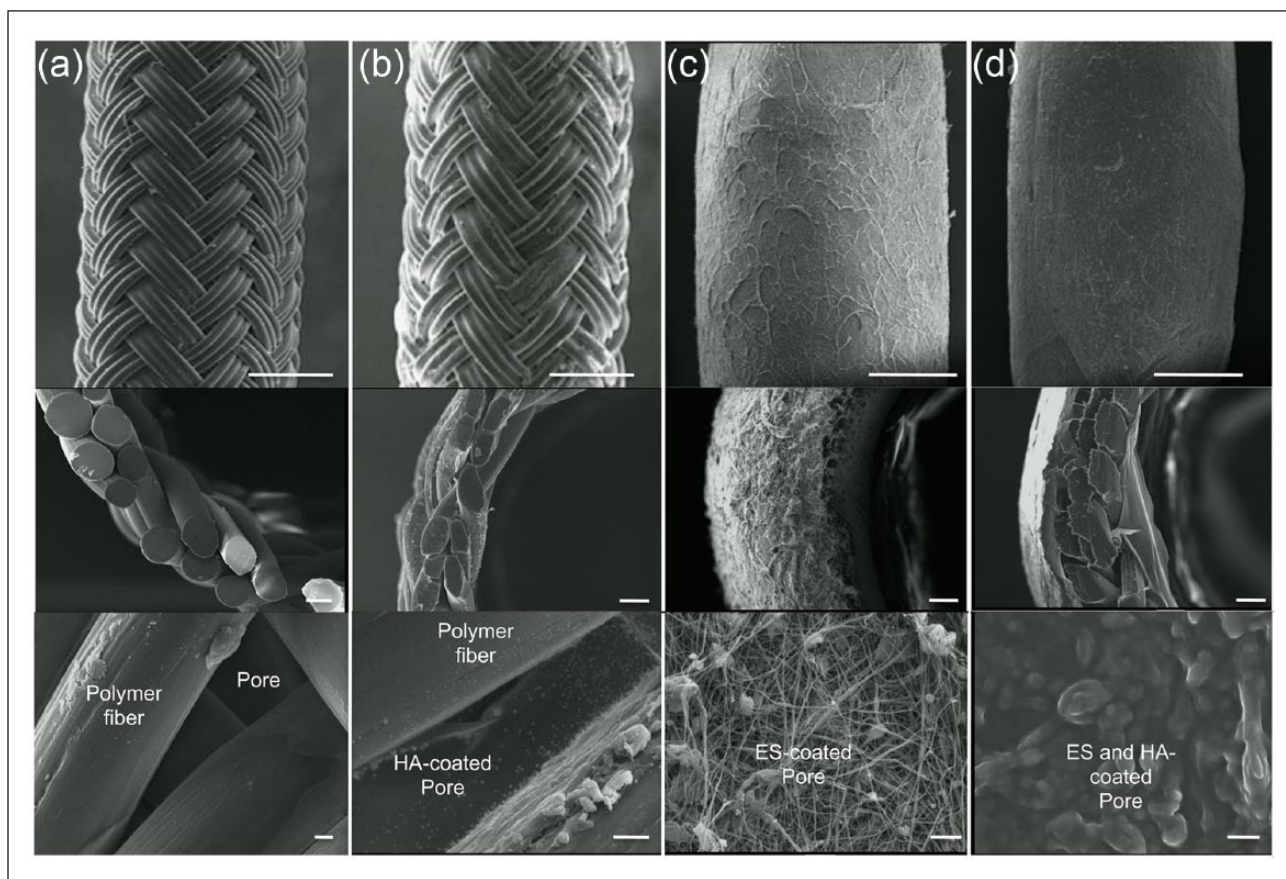


**Figure 4.** SEM images of conduit surface from side view (top panel, scale bar 1 mm), cross-sectional (end) view showing conduit wall thickness (middle panel, scale bar 100  $\mu\text{m}$ ), and a single pore area (bottom panel, scale bar 10  $\mu\text{m}$ ) and (a) uncoated braid (Group 1), (b) HA-coated braid (Group 2), (c) electrospun (ES) mat-coated braid (Group 3), and (d) ES and HA-coated braid (Group 4).

diffusion and minimize fibrotic and inflammatory cell infiltration.<sup>30,31,50</sup> E0000 braided conduits have pore dimensions ranging from 20 to 140  $\mu\text{m}$  with an average pore size of  $65 \pm 19 \mu\text{m}$  and are therefore susceptible to tissue infiltration. To address this potential problem, we developed temporary micro or nanoporous barrier coatings that allow for nutrient exchange, but reduce the ability of non-nerve cells to infiltrate into the conduit and disrupt regeneration.

Three conduit coatings were explored (Figure 4): a hydrogel coating consisting of cross-linked HA, a layer of electrospun E1001(1k) applied on the surface of the conduit, and a combination of the electrospun layer subsequently coated with HA. We used a high molecular weight and PEGDA cross-linked version of HA that we found to repel the attachment of fibroblasts (data not shown). The PEGDA cross-linked HA hydrogels are reported to be stable for 4–8 weeks in-vivo<sup>51</sup> but to our knowledge have not been used in this manner as a nerve conduit coating.

The secondary coating methods provided varying degrees of coverage on the macropores of braided conduits. The thin HA coating was nanoporous, while the

electrospun layer was microporous, with an average thickness of  $292 \pm 39 \mu\text{m}$ , fiber diameter of  $0.26 \pm 0.06 \mu\text{m}$ , and pore size of  $2.02 \mu\text{m}$ . The pore size was calculated using the equation derived by Sampson,<sup>52</sup> assuming a pore fraction of 0.85. To apply a coating of HA on top of the electrospun fiber mats, the conduits were sonicated while dipcoating them into a solution of HA. This treatment facilitated the diffusion of the HA hydrogel through the electrospun fiber mat and thoroughly coat around the fibers of the mat and the underlying conduit to create an apparently non-porous barrier. The electrospun layer shrank upon coating with the HA hydrogel to a final thickness of  $54 \pm 9 \mu\text{m}$ . Compression, bending, and tensile tests indicated that these coatings did not significantly change the mechanical properties of the braided conduits (data not shown).

#### Assessment of regeneration of the rat sciatic nerve

To evaluate the basic capacity to support nerve regeneration, E0000 braided conduits were tested in the

well-described 1 cm gap rat sciatic nerve injury model.<sup>36,37</sup> Treatment groups included the uncoated braided conduit (n=7) (Group 1), braided conduits coated with HA (n=7) (Group 2), braided conduits coated with the electrospun E1001(1k) polymer fiber mats (n=4) (Group 3), and braided conduits coated sequentially with the electrospun E1001(1k) polymer followed by HA (n=4) (Group 4). A control group of an autograft (n=7) inverted within the injury site was used (Group 5) and the regenerated nerves of all five groups were collected after 16 weeks.

### *Histomorphometric analysis of explanted nerve*

Sections of the regenerated nerve segments from the center of conduits showed that all test conduits supported regeneration of axons, but significant variation was observed (Figure 5). Uncoated conduits (Group 1), conduits having an electrospun fiber coating (Group 3), and conduits having an electrospun fiber coating plus an HA coating (Group 4) all exhibited evidence of fibrous tissue infiltration that disrupted the formation of densely packed nerve bundles and prevented the formation of a well-defined epineurium. Only the HA-coated conduits (Group 2) supported the formation of rounded and densely packed nerve cables with tightly packed fascicles and axons. Regenerated nerves within the HA-coated conduits (Group 2) all appeared to have formed an epineurial layer and resembled most closely the histomorphological appearance of the nerve bundles formed in autologous grafts (Group 5). Regenerated nerves within autologous grafts were, as expected, highly organized with a mature epineurium.

Based on these histomorphological findings, we concluded that among all barrier coatings, only the cell-repellent cross-linked HA coating (Group 2) was able to reduce the infiltration of fibrous tissue sufficiently to allow for the regeneration of healthy looking nerve tissue. It was a surprising finding that the tightly packed electrospun mats used in Group 3, and even the combination of electrospun mats and HA coating (Group 4) did not prevent significant cell infiltration into the conduit (see Figure 5 for details).

Histomorphometric characterization showed that the area occupied by myelinated axons was largest in uncoated braided conduits (Group 1), which was comparable to autologous grafts (Figure 6). HA-coated conduits (Group 2) showed the next largest myelinated area, followed by conduits of Group 4 and lastly by conduits of Group 3. In contrast, the axonal density was the highest in Group 2 conduits and lowest in Group 1 conduits, confirming that HA-coated conduits contained densely regenerated nerve cables while uncoated braided conduits have large but loosely packed nerve cables (Figure 6(b)). Assessment of axonal myelination by measuring the G-ratio showed the smallest G-ratio was obtained by autologous conduits (Group 5), with all other groups having significantly larger

G-ratios. These results show that different outcome measures provide different trends and illustrate the need to explore multiple outcome factors when assessing the histological features of regenerated nerve cables.

In comparison to the autologous grafts (Group 5), HA-coated conduits (Group 2) had a greater number of axons packed per unit area although these axons were less mature (larger G-ratio, thinner myelin sheaths). One may speculate that over longer time periods, the axons in the HA-coated conduit group will likely mature further. Based on the histomorphological evaluation of the regenerated nerve cables, the conduits of Group 2 (HA-coated conduits) seem to provide the least amount of fibrous tissue infiltration and the best milieu for nerve regeneration.

### *Muscle weight*

In contrast to the histomorphological analysis of regenerated nerve cables, muscle weight is a functional outcome measure that is directly related to the ability of a conduit to restore mobility to an injured animal. Following sciatic nerve bisection, the TA and gastrocnemius muscles innervated by branches of this nerve atrophy. Regaining of muscle weight on the operated side after nerve conduit implantation is indicative of recovery. These muscles were harvested from both hind limbs, and wet weights at the end of the 16-week recovery period were plotted (Figure 7). Muscle weight recovery of the injured side as compared to the healthy side was the greatest with autologous graft (Group 5), followed by the HA-coated braided conduits (Group 2). Group 2 conduits lead to significantly higher TA muscle weight recovery than any of the other test groups. Improved TA muscle weight recovery with the HA-coated braided conduits correlates with the higher regenerated axon density in this group compared to uncoated conduits and is, in our opinion, due to limiting the degree of fibrous tissue infiltration and subsequent formation of an epineurial layer in these conduits.

### *Electrophysiology*

Electrophysiological measurement of nerve conduction through the defect is another measure of functional nerve regeneration. We recorded the CMAP supramaximal amplitude and latency of the peroneal and tibial nerves (Figure 8). For both tibial and peroneal CMAP, the earliest post-operative CMAP signals were detected by 8 weeks for the autografts and 12 weeks for the conduit groups. 37% of the CMAP signal was recovered in the autograft group at the 16-week endpoint, which displayed the largest amplitude among all treatment groups (Figure 8(a) and (c)). Among the conduit groups, HA-coated braided conduits (Group 2) had the highest CMAP amplitudes with approximately 14% of the CMAP signal recovered at the 16-week endpoint.

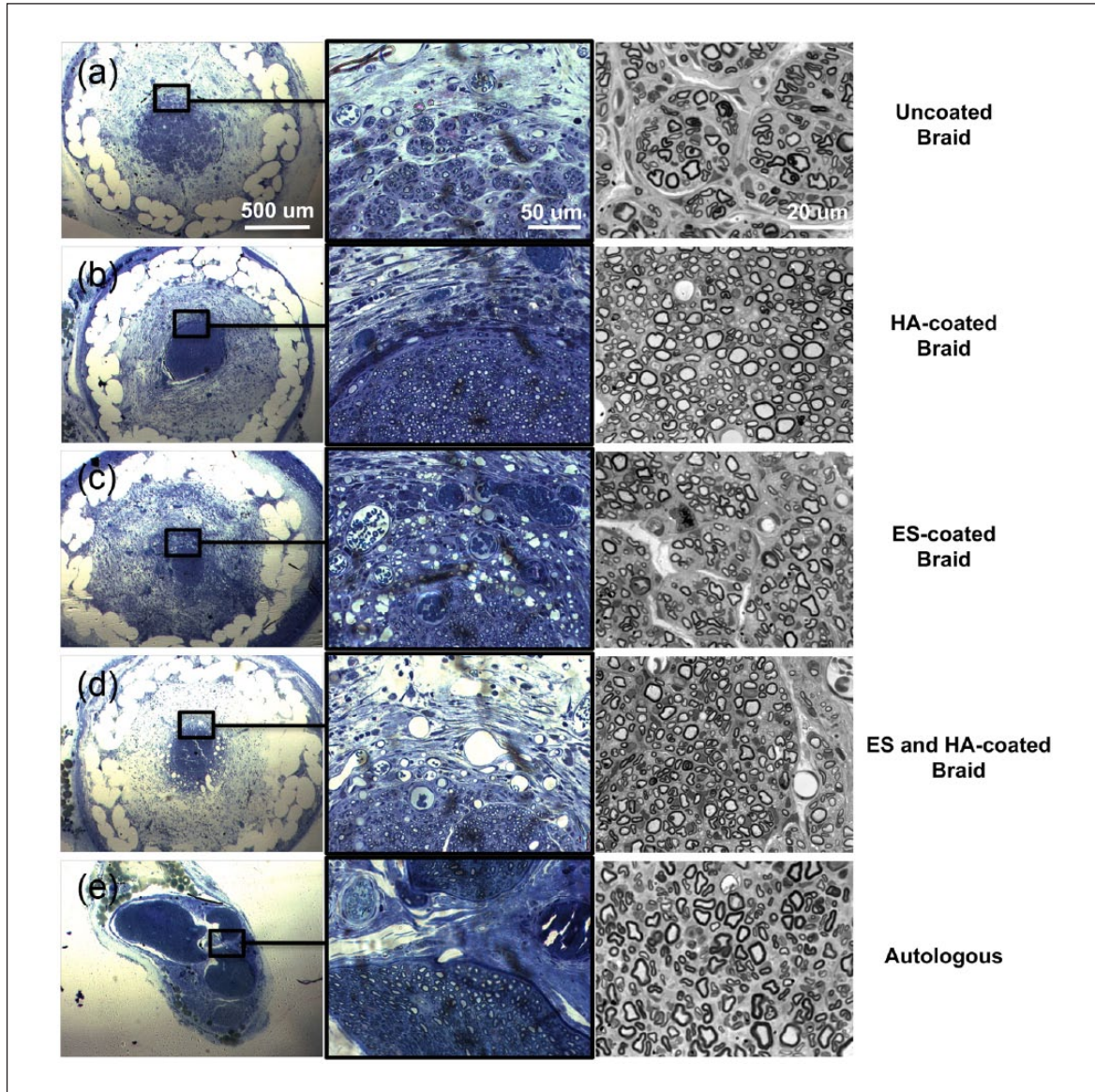


**Figure 5.** Toluidine blue stained  $1\ \mu\text{m}$  thick cross-sections of conduits explanted after 16 weeks in-vivo.  $5\times$  images (left column) show the whole conduit and nerve cable (dark stain), with varying numbers of myelinated axons and axon bundles as well as blood vessels and fibrotic tissue in braided conduits,  $40\times$  images (middle column) show the interface between axonal tissue and surrounding luminal area, and  $100\times$  images (right column) show representative high magnification images used in histomorphometric measurements. (a) Uncoated braid (Group 1), (b) HA-coated braid (Group 2), (c) electrospun (ES) mat-coated braid (Group 3), (d) ES and HA-coated braid (Group 4), and (e) autologous graft (Group 5). Regenerated tissue within Group 1 conduits showed many regenerated axons within loosely organized fascicles. A considerable amount of non-nerve tissue with a fibrous appearance was present. Similar features were noted for nerves that regenerated within braided conduits of Groups 3 and 4. The nerve cables in Groups 3 and 4 conduits were smaller in size and variable in the presence of a boundary between axonal area and the surrounding tissue. This result was surprising and suggests that the electrospun mat surrounding the braided conduit may have facilitated fibrous tissue infiltration. In contrast, the HA-coated conduits (Group 2) all showed rounded and densely packed nerve cables with tightly packed fascicles and axons and a well-formed epineurium. Regenerated nerves in Group 2 conduits were similar in histomorphological appearance to regenerated nerves within autologous grafts.

Improvement in functional regeneration is evident by the inverse correlation between CMAP latency and amplitudes. Accordingly, the autograft group had the lowest peroneal and tibial latency values at 16 weeks indicating a more rapid signal conduction (Figure 8(b) and (d)).

Observed latency values were equivalent for the braided conduit groups with the exception of the ES-coated conduits (Group 3), which displayed longer latencies, in agreement with fewer axons and greater G-ratio observed in the histology of this group.

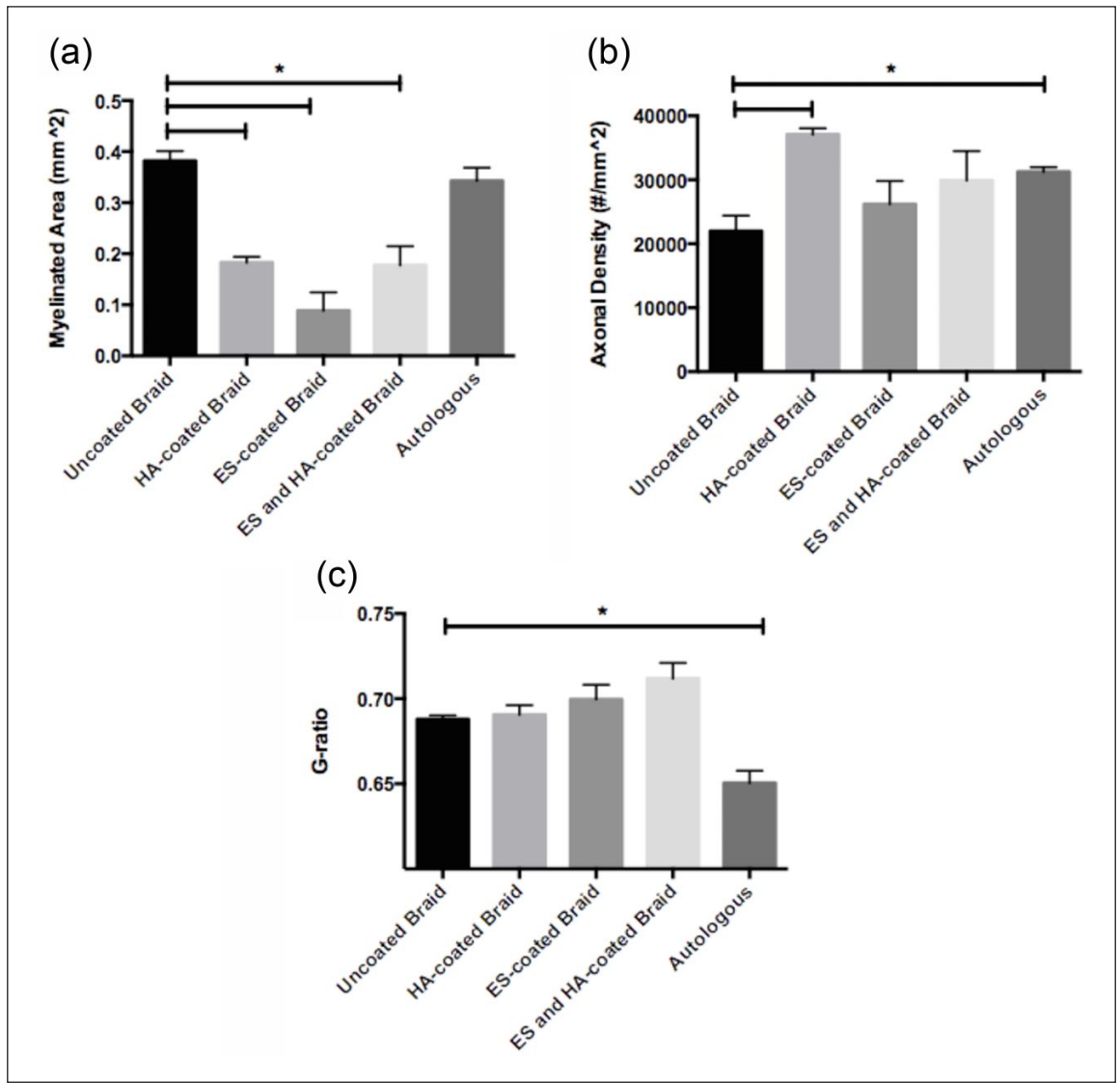


**Figure 6.** Nerve histomorphometry: (a) the total surface area of the myelinated axonal tissue, (b) the density of the myelinated nerve fibers, and (c) G-ratio; the ratio of inner axonal diameter to the total outer diameter. Data are represented as mean ± SE.

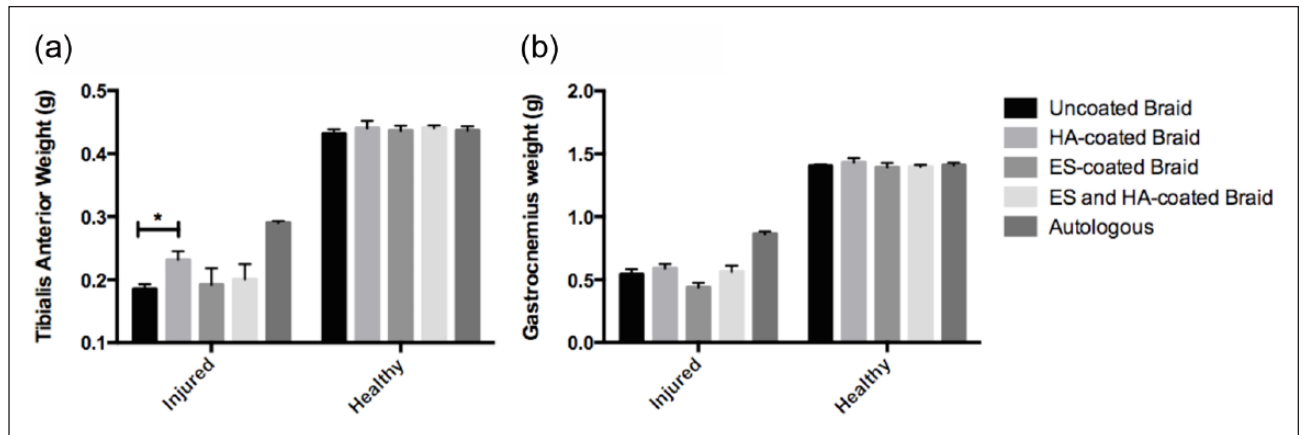


**Figure 7.** The ratio of the injured muscle weight (operated side) to the healthy muscle weight (contralateral side) of the (a) tibialis anterior and (b) gastrocnemius muscles 16 weeks post-op. Data are represented as mean ± SE.

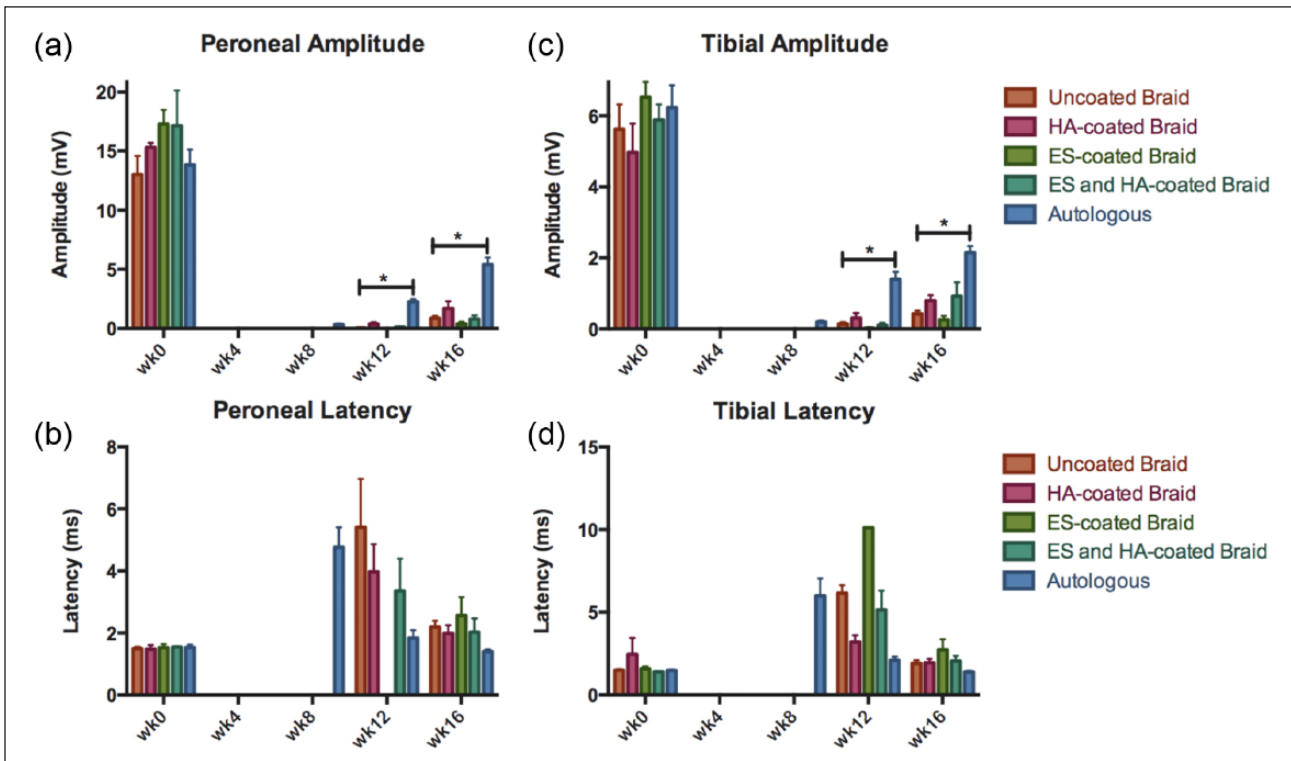


**Figure 8.** Electrophysiological measurements of pre- and post-operative amplitude (top row) and latency (bottom row) for the (a, b) tibial nerve and (c, d) peroneal nerve. Data are represented as mean  $\pm$  SE.

## Conclusion

Functional outcome measures in our study (electrophysiology and muscle weight) appear to support the histomorphological findings, indicating a major role of porosity and cell infiltration in hindering nerve recovery following injury. Perhaps most surprising result was the failure of the densely packed electrospun fiber coatings (with or without HA) to prevent the infiltration of non-nervous tissue into the lumen of the conduit. Our unpublished in-vitro experience with mats similar to those used here is that seeded cells rarely penetrate further than 60–80  $\mu\text{m}$ . However, this study found that in-vivo conduits coated with electrospun fiber mats became enriched with fibrous tissue. We believe that the extensive cell friendly surface area offered by the mats overwhelmed the cell-repellent properties of HA in Group 4 conduits. In addition, the conduit material (E0000) and the fiber mat material (E1001(1k)) favored protein adsorption and cellular attachment.<sup>33,35</sup>

We further conclude that the enhancement of nerve regeneration in HA-coated conduits (Group 2) compared to uncoated conduits (Group 1) is primarily due to the HA coating acting as a cell-repulsive barrier. However, HA is a highly adaptable material and has been used as a “filler” material for conduits with positive results,<sup>53,54</sup> raising the possibility that nerve regeneration was enhanced by the activity of HA directly on the nerves and independently of

barrier functions. However, the poor regeneration supported by braided conduits coated with an electrospun layer and HA suggests that having this HA hydrogel in the vicinity of the nerve is insufficient to positively affect regeneration, and the barrier function of HA may have been overcome by the tissue infiltration into the electrospun barrier upon degradation of the HA layer. Going forward, we anticipate that changes to the HA-coatings will lead to further enhancements of nerve regeneration using braided conduits. Studies are ongoing to achieve this by increasing the number of HA dipcoating steps, modifying hydrogel composition and cross-link density, and improving the sterilization method to maintain stability and integrity of the HA-coated conduits.

While it is implicit that conduits for long nerve gaps need to be supplemented with bioactive components (i.e. cells, growth factors, peptides, axonal constructs), the prerequisite for the development of these devices is the development of a long, flexible, kink-resistant, permeable, and degradable synthetic outer conduit that will provide sufficient mechanical support and perfusion throughout the period of nerve regeneration. While braided conduits are promising because of their kink-resistance, we have shown here that the high level of porosity associated with the braiding process facilitates the infiltration of scar tissue into the conduit that will adversely affect nerve recovery. We have overcome this

problem by developing a secondary barrier coating based on a HA-derived hydrogel to control the porosity of the braided conduits. Since HA-coated braided conduits significantly improved the level of functional nerve recovery as judged by several functional outcome measures as compared with uncoated conduits or conduits coated with electrospun fiber mats, we conclude that braided conduits in conjunction with HA-hydrogel-based barrier coatings are a promising, new technology to help improve peripheral nerve regeneration.

### Acknowledgements

The authors would like to thank Dr Anthony Windebank and Dr Huan Wang from Mayo Clinic (Rochester, MN) for their guidance in training our group with the sciatic nerve injury model and helpful discussions regarding outcomes, and Dr Jack Hershey from Rutgers University for help with animal surgeries and manuscript review. The authors also thank Dr Glenn Prestwich (University of Utah) and Dr Tom Zarembinski (Biotime, Inc.) for supplying the HA hydrogels, Dr Ijaz Ahmed for preparation of the tissue samples and The Natural Sciences and Engineering Research Council of Canada (NSERC) for BA Clements' postdoctoral training grant.

### Declaration of conflicting interests

The author(s) declared no potential conflicts of interest with respect to the research, authorship, and/or publication of this article.

### Funding

The author(s) disclosed receipt of the following financial support for the research, authorship, and/or publication of this article: This research was sponsored by the Armed Forces Institute of Regenerative Medicine award number W81XWH-08-2-0034. The US Army Medical Research Acquisition Activity, 820 Chandler Street, Fort Detrick MD 21702-5014 is the awarding and administering acquisition office. The content of the article does not necessarily reflect the position or the policy of the Government, and no official endorsement should be inferred. Research was conducted in compliance with the Animal Welfare Act Regulations and other Federal statutes relating to animals and experiments involving animals and adheres to the principles set forth in the Guide for Care and Use of Laboratory Animals, National Research Council, 1996. This work was also supported by the Center for Military Biomaterials Research (CeMBR) award number W81XWH-04-2-0031 and the New Jersey Center for Biomaterials at Rutgers University.

### References

1. Daly W, Yao L, Zeugolis D, et al. A biomaterials approach to peripheral nerve regeneration: bridging the peripheral nerve gap and enhancing functional recovery. *J R Soc Interface* 2012; 9: 202–221.
2. De Ruitter GC, Malessy MJ, Yaszemski MJ, et al. Designing ideal conduits for peripheral nerve repair. *Neurosurg Focus* 2009; 26: E5.
3. Henry EW, Chiu TH, Nyilas E, et al. Nerve regeneration through biodegradable polyester tubes. *Exp Neurol* 1985; 90: 652–676.
4. Belkas JS, Munro CA, Shoichet MS, et al. Peripheral nerve regeneration through a synthetic hydrogel nerve tube. *Restor Neurol Neuros* 2005; 23: 19–29.
5. Midha R, Munro CA, Dalton PD, et al. Growth factor enhancement of peripheral nerve regeneration through a novel synthetic hydrogel tube. *J Neurosurg* 2003; 99: 555–565.
6. Den Dunnen WFA, Meek MF, Robinson PH, et al. Peripheral nerve regeneration through P(DLLA-epsilon-CL) nerve guides. *J Mater Sci Mater Med* 1998; 9: 811–814.
7. Meek MF. More than just sunshine with implantation of resorbable (p(DLLA-epsilon-CL)) biomaterials. *Biomed Mater Eng* 2007; 17: 329–334.
8. Kim JH, Kang TJ and Yu W-R. Mechanical modeling of self-expandable stent fabricated using braiding technology. *J Biomech* 2008; 41: 3202–3212.
9. Ahlhelm F, Kaufmann R, Ahlhelm D, et al. Carotid artery stenting using a novel self-expanding braided nickel-titanium stent: feasibility and safety porcine trial. *Cardiovasc Inter Rad* 2009; 32: 1019–1027.
10. Toba T, Nakamura T, Shimizu Y, et al. Regeneration of canine peroneal nerve with the use of a polyglycolic acid-collagen tube filled with laminin-soaked collagen sponge: a comparative study of collagen sponge and collagen fibers as filling materials for nerve conduits. *J Biomed Mater Res* 2001; 58: 622–630.
11. Kiyotani T, Teramachi M, Takimoto Y, et al. Nerve regeneration across a 25-mm gap bridged by a polyglycolic acid-collagen tube: a histological and electrophysiological evaluation of regenerated nerves. *Brain Res* 1996; 740: 66–74.
12. Kiyotani T, Nakamura T, Shimizu Y, et al. Experimental study of nerve regeneration in a biodegradable tube made from collagen and polyglycolic acid. *ASAIO J* 1995; 41: M657–M661.
13. Inada Y, Morimoto S, Moroi K, et al. Surgical relief of causalgia with an artificial nerve guide tube: successful surgical treatment of causalgia (Complex Regional Pain Syndrome Type II) by in situ tissue engineering with a polyglycolic acid-collagen tube. *Pain* 2005; 117: 251–258.
14. Ichihara S, Inada Y, Nakada A, et al. Development of new nerve guide tube for repair of long nerve defects. *Tissue Eng Part C Methods* 2009; 15: 387–402.
15. Bini TB, Gao S, Xu X, et al. Peripheral nerve regeneration by microbraided poly(L-lactide-co-glycolide) biodegradable polymer fibers. *J Biomed Mater Res A* 2004; 68: 286–295.
16. Bini TB, Gao S, Wang S, et al. Development of fibrous biodegradable polymer conduits for guided nerve regeneration. *J Mater Sci Mater Med* 2005; 16: 367–375.
17. Lu MC, Huang YT, Lin JH, et al. Evaluation of a multi-layer microbraided polylactic acid fiber-reinforced conduit for peripheral nerve regeneration. *J Mater Sci Mater Med* 2009; 20: 1175–1180.
18. Yoshitani M, Fukuda S, Itoi S, et al. Experimental repair of phrenic nerve using a polyglycolic acid and collagen tube. *J Thorac Cardiovasc Surg* 2007; 133: 726–732.
19. Henry M, Klonaris C, Amor M, et al. State of the art: which stent for which lesion in peripheral interventions? *Tex Heart Inst J* 2000; 27: 119–126.

20. Freitas AFDP, de Araujo MD, Zu WW, et al. Development of weft-knitted and braided polypropylene stents for arterial implant. *J Text I* 2010; 101: 1027–1034.
21. Kim J, Magno MH, Alvarez P, et al. Osteogenic differentiation of pre-osteoblasts on biomimetic tyrosine-derived polycarbonate scaffolds. *Biomacromolecules* 2011; 12: 3520–3527.
22. Kohn J and Zeltinger J. Degradable, drug-eluting stents: a new frontier for the treatment of coronary artery disease. *Expert Rev Med Devices* 2005; 2: 667–671.
23. Lewitus D, Vogelstein RJ, Zhen G, et al. Designing tyrosine-derived polycarbonate polymers for biodegradable regenerative type neural interface capable of neural recording. *IEEE Trans Neural Syst Rehabil Eng* 2011; 19: 204–212.
24. Macri LK, Sheihet L, Singer AJ, et al. Ultrafast and fast bioerodible electrospun fiber mats for topical delivery of a hydrophilic peptide. *J Control Release* 2012; 161: 813–820.
25. Tangpasuthadol V, Pendharkar SM, Peterson RC, et al. Hydrolytic degradation of tyrosine-derived polycarbonates, a class of new biomaterials. Part II: 3-yr study of polymeric devices. *Biomaterials* 2000; 21: 2379–2387.
26. Ertel SI and Kohn J. Evaluation of a series of tyrosine-derived polycarbonates as degradable biomaterials. *J Biomed Mater Res* 1994; 28: 919–930.
27. Nakamura T, Inada Y, Fukuda S, et al. Experimental study on the regeneration of peripheral nerve gaps through a polyglycolic acid-collagen (PGA-collagen) tube. *Brain Res* 2004; 1027: 18–29.
28. Matsumoto K, Ohnishi K, Kiyotani T, et al. Peripheral nerve regeneration across an 80-mm gap bridged by a polyglycolic acid (PGA)-collagen tube filled with laminin-coated collagen fibers: a histological and electrophysiological evaluation of regenerated nerves. *Brain Res* 2000; 868: 315–328.
29. Jenq CB, Jenq LL and Coggeshall RE. Nerve regeneration changes with filters of different pore size. *Exp Neurol* 1987; 97: 662–671.
30. Vleggeert-Lankamp CL, De Ruiters GC, Wolfs JF, et al. Pores in synthetic nerve conduits are beneficial to regeneration. *J Biomed Mater Res A* 2007; 80: 965–982.
31. Chamberlain LJ, Yannas IV, Arrizabalaga A, et al. Early peripheral nerve healing in collagen and silicone tube implants: myofibroblasts and the cellular response. *Biomaterials* 1998; 19: 1393–1403.
32. Engelberg I and Kohn J. Physico-mechanical properties of degradable polymers used in medical applications: a comparative study. *Biomaterials* 1991; 12: 292–304.
33. Magno MHR, Kim J, Srinivasan A, et al. Synthesis, degradation and biocompatibility of tyrosine-derived polycarbonate scaffolds. *J Mater Chem* 2010; 20: 8885–8893.
34. Florek CA. *A synthetic biomaterials approach to the prevention of postsurgical adhesions in neurosurgery. The Graduate Program in Biomedical Engineering*. New Brunswick, NJ: Rutgers, The State University of New Jersey, 2010, p. 189.
35. Ezra M, Bushman J, Shreiber DI, et al. Enhanced femoral nerve regeneration after tubulization with a tyrosine-derived polycarbonate terpolymer: effects of protein adsorption and independence of conduit porosity. *Tissue Eng Part A* 2013; 20(3–4): 518–528.
36. Rui J, Dadsetan M, Runge MB, et al. Controlled release of vascular endothelial growth factor using poly-lactic-co-glycolic acid microspheres: in-vitro characterization and application in polycaprolactone fumarate nerve conduits. *Acta Biomater* 2012; 8: 511–518.
37. De Ruiters GC, Malessy MJ, Alaid AO, et al. Misdirection of regenerating motor axons after nerve injury and repair in the rat sciatic nerve model. *Exp Neurol* 2008; 211: 339–350.
38. Irintchev A, Draguhn A and Wernig A. Reinnervation and recovery of mouse soleus muscle after long-term denervation. *Neuroscience* 1990; 39: 231–243.
39. Harte AM and Fleck NA. Deformation and failure mechanisms of braided composite tubes in compression and torsion. *Acta Materialia* 2000; 48: 1259–1271.
40. Li ST, Archibald SJ, Krarup C, et al. Peripheral nerve repair with collagen conduits. *Clin Mater* 1992; 9: 195–200.
41. Archibald SJ, Krarup C, Shefner J, et al. A collagen-based nerve guide conduit for peripheral nerve repair: an electrophysiological study of nerve regeneration in rodents and nonhuman primates. *J Comp Neurol* 1991; 306: 685–696.
42. Yao L, Billiar KL, Windebank AJ, et al. Multichanneled collagen conduits for peripheral nerve regeneration: design, fabrication, and characterization. *Tissue Eng Part C Methods* 2010; 16: 1585–1596.
43. Yoshii S and Oka M. Collagen filaments as a scaffold for nerve regeneration. *J Biomed Mater Res* 2001; 56: 400–405.
44. Topp KS and Boyd BS. Structure and biomechanics of peripheral nerves: nerve responses to physical stresses and implications for physical therapist practice. *Phys Ther* 2006; 86: 92–109.
45. Topp KS and Boyd BS. Peripheral nerve: from the microscopic functional unit of the axon to the biomechanically loaded macroscopic structure. *J Hand Ther* 2012; 25: 142–151.
46. Bueno FR and Shah SB. Implications of tensile loading for the tissue engineering of nerves. *Tissue Eng Pt B: Rev* 2008; 14: 219–233.
47. Kwan MK, Wall EJ, Massie J, et al. Strain, stress and stretch of peripheral nerve. Rabbit experiments in vitro and in vivo. *Acta Orthop Scand* 1992; 63: 267–272.
48. Rydevik BL, Kwan MK, Myers RR, et al. An in vitro mechanical and histological study of acute stretching on rabbit tibial nerve. *J Orthop Res* 1990; 8: 694–701.
49. Hooper KA, Nickolas TL, Yurkow EJ, et al. Characterization of the inflammatory response to biomaterials using a rodent air pouch model. *J Biomed Mater Res* 2000; 50: 365–374.
50. Jenq CB and Coggeshall RE. Nerve regeneration through holey silicone tubes. *Brain Res* 1985; 361: 233–241.
51. Liu Y, Shu XZ and Prestwich GD. Osteochondral defect repair with autologous bone marrow-derived mesenchymal stem cells in an injectable, in situ, cross-linked synthetic extracellular matrix. *Tissue Eng* 2006; 12: 3405–3416.
52. Sampson WW. A multiplanar model for the pore radius distribution in isotropic near-planar stochastic fibre networks. *J Mater Sci* 2003; 38: 1617–1622.
53. Wang KK, Nemeth IR, Seckel BR, et al. Hyaluronic acid enhances peripheral nerve regeneration in vivo. *Microsurgery* 1998; 18: 270–275.
54. Mohammad JA, Warnke PH, Pan YC, et al. Increased axonal regeneration through a biodegradable amniotic tube nerve conduit: effect of local delivery and incorporation of nerve growth factor/hyaluronic acid media. *Ann Plast Surg* 2000; 44: 59–64.